Journal of Physiology (1995), **485.2**, *pp.* 419–435

Whole-cell and single-channel currents activated by GABA and glycine in granule cells of the rat cerebellum

Makoto Kaneda, Mark Farrant* and Stuart G. Cull-Candy

Department of Pharmacology, University College London, Gower Street, London WC1E 6BT, UK

1. Patch-clamp methods have been used to characterize GABA- and glycine-activated channels and spontaneous synaptic currents in granule cells in thin cerebellar slices from 7- to 20-day-old rats.

2. All granule cells responded to 10 μM GABA, while ~60% responded to 100 μM glycine. With repeated agonist application, whole-cell responses to GABA, but not those to glycine, declined over a period of minutes unless the pipette solution contained Mg-ATP.

3. Whole-cell concentration–response curves gave EC_{50} values of 45·2 and 99·6 μM and Hill slopes of 0·94 and 2·6 for GABA and glycine, respectively. At saturating concentrations, currents evoked by GABA were fivefold larger than those evoked by glycine.

4. Whole-cell current–voltage (I–V) relationships of GABA- and glycine-activated currents reversed close to the predicted Cl^- equilibrium potential. Partial replacement of intracellular Cl^- with F^- shifted the GABA reversal potential to a more negative value. 'Instantaneous' I–V relationships produced by ionophoretic application of GABA were linear, while 'steady-state' I–V relationships produced by ramp changes in potential showed outward rectification. For glycine, 'steady-state' I–V plots were linear.

5. Responses to GABA were blocked by the $GABA_A$ receptor antagonists bicuculline (15 μM), SR-95531 (10 μM) and picrotoxinin (100 μM), while responses to glycine were selectively blocked by strychnine (200 nM), indicating the presence of two separate receptor types.

6. In outside-out membrane patches, GABA opened channels with conductances of 16 and 28 pS. The proportion of openings to each of the conductances varied between patches, possibly indicating the activation of two distinct channel types. Glycine-activated single-channel currents had conductances of 32, 55 and 104 pS. Single-channel I–V relationships were linear.

7. Spontaneous synaptic currents with a rapid rise time and biexponential decay were present in more than half of the cells examined. These currents were eliminated by bicuculline (15 μM) or SR-95531 (10 μM) and were greatly reduced in frequency by tetrodotoxin (TTX; 300 nM), suggesting that they were mediated by GABA and arose from spontaneous activity in Golgi interneurones. In granule cells where this spontaneous synaptic activity was apparent, glycine and low concentrations of GABA increased the frequency of the synaptic currents.

8. In many cells a bicuculline-sensitive 'background current noise' was seen in the presence of glutamate antagonists and TTX. Power spectra of this background noise (following subtraction of noise recorded in the presence of bicuculline) were fitted with the sum of two Lorentzian curves and gave an estimated single-channel conductance of 13·7 pS, comparable to the value of 15·3 pS obtained from spectra of noise produced by externally applied GABA (10 μM).

9. Our results indicate that granule cells express distinct GABA- and glycine-activated ion channels. Although both amino acids are known to be present in the terminals of Golgi neurones that form inhibitory inputs to granule cells, spontaneous inhibitory postsynaptic currents (IPSCs) in granule cells appear to be mediated exclusively by GABA.

* To whom correspondence should be addressed.

Granule cells of the cerebellum receive synaptic input from Golgi interneurones, which in the adult give rise to inhibition mediated by γ-aminobutyric acid (GABA) (Bisti, Iosif, Marchesi & Strata, 1971). The ease with which granule cells can be isolated, together with their well-documented development and restricted synaptic input, has made them an attractive cell type in which to study the expression, organization and developmental regulation of $GABA_A$ receptors. However, until recently (Puia, Costa & Vicini, 1994), the functional properties of $GABA_A$ receptors in granule cells have only been studied in explant or dissociated cultures (Cull-Candy & Ogden, 1985; Vicini, Wrobleski & Costa, 1986; Kilić, Moran & Cherubini, 1993; Robello, Amico & Cupello, 1993; Maconochie, Zempel & Steinbach, 1994), under conditions that may influence the expression of $GABA_A$ receptor subunit mRNAs (Bovolin, Santi, Puia, Costa & Grayson, 1992; Beattie & Siegel, 1993; Thompson & Stephenson, 1994) and hence the characteristics of the GABA receptors.

Golgi cells also accumulate and release the inhibitory neurotransmitter glycine (Wilkin, Csillag, Balázs, Kingsbury, Wilson & Johnson, 1981; Morales & Tapia, 1987). Indeed, most Golgi cell terminals exhibit both GABA- and glycine-like immunoreactivity (Ottersen, Storm-Mathisen & Somogyi, 1988), although the functional significance of this remains unclear. While there is immunohistochemical evidence for glycine receptors on some granule cell dendrites (Triller, Cluzeaud & Korn, 1987), in the adult cerebellum there is only a low level of glycine receptor expression (Araki, Yamano, Murakami, Wanaka, Betz & Tohyama, 1988) and no detectable glycine-sensitive strychnine binding (Zarbin, Wamsley & Kuhar, 1981).

In the present study, we have examined the properties of $GABA_A$-receptor channels and inhibitory synaptic currents (IPSCs) in granule cells, and investigated whether these cells also express functional glycine receptors. As our aim has been to obtain information about receptors normally present *in vivo*, we have used thin cerebellar slices rather than cultured cells. Our results demonstrate that granule cells possess both $GABA_A$ and glycine receptors, and that these are linked to distinct anion channels. Despite the fact that glycine is present in the terminals of Golgi interneurones, we find that IPSCs in granule cells are mediated exclusively by GABA. Some of our results have been published in a preliminary report (Kaneda, Farrant & Cull-Candy, 1994).

METHODS

Tissue and preparation

Recordings were made from granule cells of the cerebellum in parasagittal slices obtained from 7- to 20-day-old Sprague–Dawley rats. Cerebellar slices were prepared and maintained as previously described (Farrant & Cull-Candy, 1991). Briefly, rats were decapitated and their brains rapidly removed and placed in ice-cold Krebs–Henseleit 'slicing' solution. This contained (mM): NaCl, 125; KCl, 2·5; $CaCl_2$, 1; $MgCl_2$, 4; $NaHCO_3$, 26; NaH_2PO_4, 1·25; glucose, 25; and lactate, 4; pH 7·4 when bubbled with 95% O_2–5% CO_2. The bisected cerebellum was glued to the stage of a vibrating microslicer (DTK-1000, Dosaka EM Co. Ltd., Kyoto, Japan) and cut into slices 150–200 μm thick. These were transferred to an incubating chamber containing slicing solution bubbled continuously with 95% O_2–5% CO_2. Slices were maintained at 30 °C for 1 h; thereafter they were maintained at room temperature for up to 8 h before use.

Solutions and drugs

During recording, slices were continuously perfused with a solution containing (mM): NaCl, 125; KCl, 2·5; $CaCl_2$, 2; $MgCl_2$, 1; $NaHCO_3$, 26; NaH_2PO_4, 1·25; and glucose, 25; pH 7·4 when bubbled with 95% O_2–5% CO_2. The pipette solution (intracellular solution) contained (mM): CsCl, 140; NaCl, 4; $CaCl_2$, 0·5; *N*-2-hydroxyethylpiperazine-*N'*-2-ethanesulphonic acid (Hepes), 10; and ethyleneglycol-bis(β-aminoethylether)-*N,N,N',N'*-tetraacetic acid (EGTA), 5; adjusted to pH 7·3 with CsOH. In some experiments 140 mM CsCl was replaced with 110 mM CsF plus 30 mM CsCl. To prevent the progressive decline of GABA-evoked currents seen with repeated application (see Results), 2 mM Mg-ATP was added to the internal solutions.

Drugs were applied to the slice via the perfusion medium. GABA (Sigma) was also applied ionophoretically, by passing 50–100 nA of current through micropipettes (~50 MΩ) filled with 100 mM GABA (pH 4·0, with HCl) placed close to the recorded cell. A small retaining current was applied to the pipette to limit GABA leakage. In most experiments, 10 μM D-2-amino-5-phosphonopentanoic acid (D-AP5; Tocris Cookson, Bristol, UK) and 5 μM 6-cyano-7-nitroquinoxaline-2,3-dione (CNQX; Tocris Cookson) were added to the perfusion medium to prevent activation of *N*-methyl-D-aspartate (NMDA) and non-NMDA glutamate receptors, respectively. Other drugs used in the present experiments were: glycine (BDH, Poole, UK), bicuculline methobromide (Tocris Cookson), strychnine HCl (Sigma), picrotoxinin (Sigma), SR-95531 (Research Biochemicals International, Natick, MA, USA) and tetrodotoxin (TTX; Sigma).

Current recording

Whole-cell and outside-out patch recordings were made at room temperature (22–25 °C) from granule cells on the surface of the slice. Cells were viewed with Nomarski differential interference optics (Zeiss; ×40 water immersion objective, total magnification ×320–1000). Mechanical cleaning of the cell surface, to facilitate seal formation, was not required. Recordings were made using an Axopatch-1A or -1D patch-clamp amplifier (Axon Instruments). Patch pipettes were pulled from thick-walled glass (Clark Electromedical GC150F-7·5), coated with Sylgard resin (Dow Corning 184) and fire polished to a resistance of 8–12 MΩ when filled with intracellular solution. Cell capacitance (3·7 ± 0·1 pF; mean ± S.E.M.; $n = 109$) series resistance (30·3 ± 1·4 MΩ) and input resistance (7·6 ± 0·6 GΩ) were measured from the amplifier and from transient currents produced by 10 mV hyperpolarizing voltage steps.

Data acquisition and analysis

Transient currents generated by hyperpolarizing voltage steps were digitized 'on-line' at 100–125 kHz (Intel 80386- or 80486-based personal computer; pCLAMP 5.5 with TL-1 interface, Axon Instruments) after filtering at 20 kHz (−3 dB). Other current data were recorded on FM tape (Racal Store 4; bandwidth DC to

1·25–5 kHz, −3 dB) or on digital audio tape (BioLogic DTR-1204; DC to 20 kHz). Peak currents of whole-cell responses to perfusion-applied agonist were measured off-line from records digitized at 1 kHz, or as displayed on a chart recorder (Kipp & Zonen BD-41).

Current–voltage relationships

I–V relationships for whole-cell currents evoked by 10 μM GABA or 100 μM glycine were generated by applying a voltage ramp to the command potential (−100 to 50 mV, 200 mV s^{-1}). The resulting currents were digitized on-line at 2 kHz after filtering at 1 kHz. *I–V* relationships were produced after subtracting the current obtained in the absence of agonist from that obtained during the steady-state response to GABA or glycine. In each condition, three or four ramps were applied at 3 s intervals and the resulting currents averaged. *I–V* relationships were also obtained from the measurement of peak current responses to ionophoretically applied GABA (digitized on-line at 5 kHz). GABA was applied for durations of 10–12 ms at 3 s intervals, 300 ms after changing to test potentials of −100 to 30 mV from a holding potential of −60 mV.

Noise analysis

For spectral analysis of GABA noise, records were digitized at 4 kHz (PDP-11/73 with a CED 502 interface, Cambridge Electronic Design, Cambridge, UK) after bandpass filtering (0·2 Hz–2 kHz; −3 dB, 8-pole Butterworth filter). Digitized records were split into sections of length $1/f_{res}$ (where f_{res} was the desired resolution, usually 2 Hz). Spectral densities for each section of data were calculated and averaged to give a mean power spectrum. A net one-sided spectrum was obtained by subtracting the mean control spectrum from the mean spectrum of agonist-induced noise. The resulting spectrum was fitted with the sum of two Lorentzian curves, each described by:

$$G(f) = G(0)/\{1 + (f/f_c)^2\},$$

where $G(f)$ is the single-sided spectral density at any given frequency, $G(0)$ is the spectral density at the zero-frequency asymptote and f_c is the cut-off frequency at which $G(f) = G(0)/2$. The area under the fitted curve is equal to the total current variance (σ^2) evoked by agonist. The single-channel current, i_{noise}, was calculated from the relationship:

$$i_{noise} = \pi\{G_1(0)f_{c1} + G_2(0)f_{c2}\}/2\,\mu_I,$$

where $G_1(0)$ and f_{c1} and $G_2(0)$ and f_{c2} are the zero-frequency asymptote and the cut-off frequencies of the fast and slow components, respectively, and μ_I is the mean agonist-induced whole-cell current. τ_{noise} was calculated from the cut-off frequencies of the fitted curves according to: $\tau_{noise} = 1/(2\pi f_c)$.

Single-channel analysis

GABA-activated single-channel currents recorded in outside-out patches were replayed from tape, filtered at 2 kHz (−3 dB, 8-pole Bessel type filter) and digitized at 10 kHz (PDP-11/73 with CED 502). Individual openings were fitted by the step response function of the recording system; a resolution of 2 × the filter rise time was subsequently imposed on the results (Colquhoun & Sigworth, 1983). The mean amplitude levels of single-channel currents were determined from fits of one or two Gaussian distributions to the cursor-fitted amplitudes. The mean open time of individually resolved events was determined from fits of one or two exponential components to distributions of the length of apparent openings. Because of their low density (see Results), glycine-activated channels were recorded in the whole-cell configuration. Records were replayed from tape, filtered at 1 kHz and digitized at 5 kHz. Mean current levels were determined from fits of Gaussian distributions to histograms of cursor-measured single-channel openings. All distributions were fitted by the method of maximum likelihood (Colquhoun & Sigworth, 1983).

RESULTS

Whole-cell currents activated by GABA and glycine

Granule cells were identified on the basis of (a) their small soma and location in the inner granular layer, and (b) their characteristically small capacitance and high input resistance (see Silver, Traynelis & Cull-Candy, 1992; Farrant, Feldmeyer, Takahashi & Cull-Candy, 1994). As shown in Fig. 1*A*, these cells responded to the application of GABA (in the presence of 300 nM TTX, 5 μM CNQX and 10 μM D-AP5) with inward currents at negative membrane potentials, as expected for the activation of Cl^- channels under our recording conditions. Similarly, in many cells glycine also evoked an inward current (Fig. 1*B*). The responses to 10 μM GABA developed rapidly and desensitized to a steady-state level, while currents evoked by 100 μM glycine took longer to reach peak amplitude, were associated with greater current noise and generally desensitized more slowly. For both agonists the extent of desensitization was variable from cell to cell. In all cases, the responses declined rapidly when agonist was removed. Very occasionally we encountered cells with a much larger capacitance, which we presume to have been Golgi interneurones. These cells were also responsive to GABA and glycine, but the currents evoked by glycine were larger than commonly seen with granule cells.

In all granule cells tested, the repeated application of GABA led to a progressive decrease in the peak current amplitude. This 'run-down' of the GABA response was examined by applying 10 μM GABA at 3 min intervals (Fig. 1*C*). The decline in response could be described by a single exponentially decaying function:

$$I_{GABA} = (I_0 - I_{ss})e^{(-t/\tau)} + I_{ss},$$

where I_{GABA} is the relative amplitude of the GABA response obtained at time t after the start of whole-cell recording, I_0 is the amplitude of the initial current ($t = 1$ min), I_{ss} is the amplitude of the GABA response at steady state and τ is the decay time constant. Data from eight cells gave a value for τ of 8·5 min and I_{ss} of 9%. A similar decline in the response to exogenous GABA during whole-cell recording has been observed in a variety of dissociated or cultured neurones (Gyenes, Farrant & Farb, 1988; Stelzer, Kay & Wong, 1988; Chen, Stelzer, Kay & Wong, 1990), including cerebellar granule cells (Robello *et al.* 1993). The present data clearly show that this phenomenon occurs in neurones in the more intact environment of a slice preparation. In accord with earlier studies, the decline in current response was prevented by

the inclusion of ATP in the intracellular solution, consistent with the suggestion that phosphorylation via protein kinase A is required for the maintenance of $GABA_A$ receptor function (Chen *et al.* 1990). As shown in Fig. 1*C*, GABA responses recorded with solutions containing 2 mM Mg-ATP showed little change in amplitude during a 30 min period. All our subsequent recordings were therefore obtained with this intracellular solution. Under these conditions, in 13- to 15-day-old rats, all cells tested responded to 10 μM GABA ($n = 75$) while 56% of cells tested responded to 100 μM glycine ($n = 64$). Currents evoked by 100 μM glycine showed no evidence of 'run-down' when recordings were made without ATP in the intracellular solution ($n = 5$; Fig. 1*D*).

Concentration dependence of GABA- and glycine-induced currents

To characterize further the GABA and glycine receptors in these cells we examined their concentration–response relationships. The lowest concentration producing a detectable current was 300 nM for GABA and 10 μM for glycine. For each cell, the peak amplitude of currents evoked by various concentrations of each agonist were

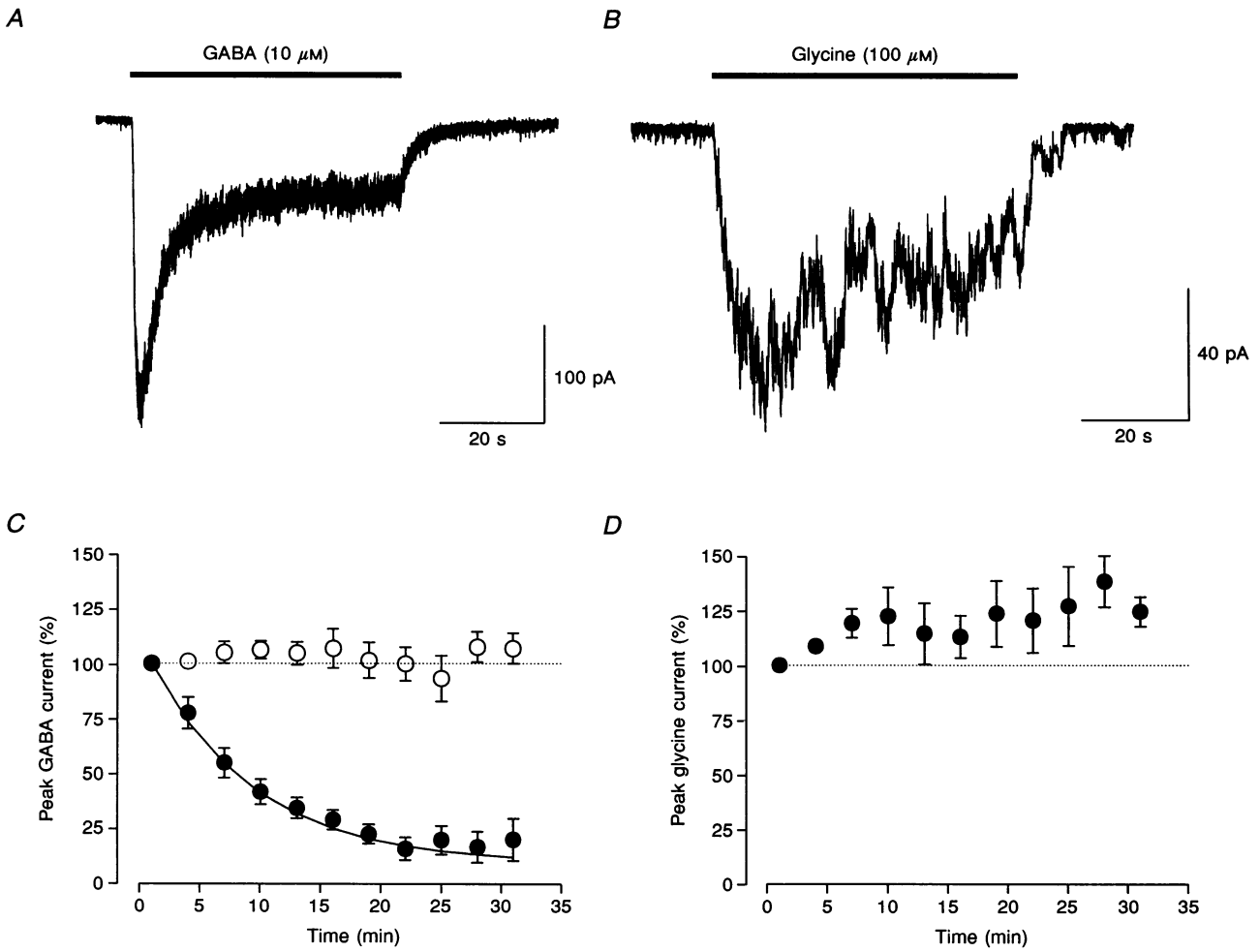

Figure 1. GABA- and glycine-evoked whole-cell currents in cerebellar granule cells

A, a representative whole-cell current produced by application of GABA (10 μM) to a cell held at −50 mV. The bar above the trace indicates the duration of GABA application. *B*, a whole-cell current produced by application of glycine (100 μM; same cell as *A*). The recordings were obtained in the presence of D-AP5 (10 μM), CNQX (5 μM) and TTX (300 nM). *C* and *D*, stability of GABA- (*C*) and glycine-evoked (*D*) currents recorded when using either an intracellular solution without added ATP (●) or a solution containing 2 mM Mg-ATP (○). In each case, currents were evoked at 3 min intervals and their peak amplitude expressed as a percentage of the current obtained 1 min after establishing the whole-cell recording. Each point represents the mean value of 4–8 (GABA) or 3–5 (glycine) observations; S.E.M. are indicated where larger than the symbol. In *C*, the continuous curve is the best fit of the data to a single exponential decay (see Results) with a time constant of 8·5 min. Currents evoked by 100 μM glycine were also stable in the presence of 2 mM Mg-ATP; the peak current for responses obtained 8–12 min after the first glycine application was 97·1 ± 4·5% ($n = 9$) of the initial response.

normalized to those evoked by 10 μM GABA and pooled data were plotted against agonist concentration (Fig. 2*A*). With increasing concentrations of GABA and glycine the whole-cell currents increased in amplitude in a sigmoidal fashion until saturation was apparent at about 1 mM. The curves were fitted (Marquardt–Levenberg algorithm, least-squares criterion) with the equation:

$$I = I_{max}/(1 + \{EC_{50}/A\}^{n_H}),$$

where I_{max} is the maximal response, A is the agonist concentration, n_H is the Hill coefficient, and EC_{50} is the concentration of agonist producing a half-maximal current response. Analysis of data from a total of eighteen cells yielded a Hill coefficient of 0·94 and an EC_{50} of 45·2 μM for GABA; corresponding values for glycine were 2·6 and 99·6 μM (11 cells). At saturating concentrations, currents evoked by GABA (1 mM; 123·3 ± 21·3 pA pF^{-1}, $n = 7$) were consistently larger than those evoked by glycine (3 mM; 26·1 ± 10·9 pA pF^{-1}, $n = 3$).

The EC_{50} determined for GABA is somewhat higher than the values of 2·3–20·7 μM for these cells in culture (Kilić *et al.* 1993; Robello *et al.* 1993; Maconochie *et al.* 1994). In our experiments no attempt was made to inhibit the possible uptake of GABA or glycine into neurones and glial cells, so the exact concentration of the agonists at their receptors is not known. In addition, desensitization was apparent at GABA concentrations above 3 μM and at glycine concentrations above 30 μM. A rapid component (time constant 5 ms) of $GABA_A$ receptor desensitization in cerebellar granule cells has recently been described (Puia *et al.* 1994). Because of the modest speed of agonist application in the present study, desensitization will take place during the rising phase of current responses but the extent of this is unknown.

Developmental changes in GABA and glycine receptor expression

During the second and third postnatal weeks the current response to GABA increased in magnitude. Figure 2*B* shows data (normalized by cell capacitance) obtained from animals aged 7, 12–15 and 20 days. At 20 days, the response to 10 μM GABA was significantly increased over that seen at day 7 and days 12–15 ($P < 0·05$; Student's t test). In contrast, during the same time period the response to 100 μM glycine did not change significantly ($P > 0·05$).

Current–voltage relationships of GABA- and glycine-induced currents

Figure 3*A* shows a family of currents produced by the ionophoretic application of GABA at potentials between −100 and +30 mV (in 10 mV steps). The relationship between peak amplitude of the currents and membrane

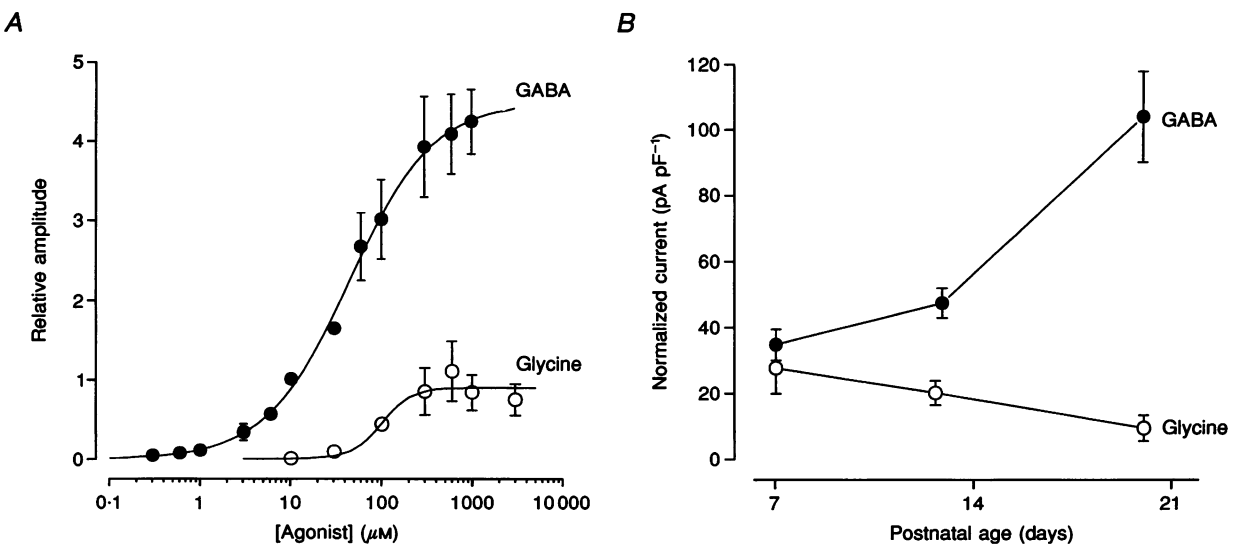

Figure 2. Concentration–response relationships and developmental changes of GABA- and glycine-evoked currents

A, plots of peak whole-cell current amplitude *versus* agonist concentration. Currents were evoked by GABA or glycine applied at 2–4 min intervals at a holding potential of −50 mV. A control response to 10 μM GABA was obtained before and after each test concentration of GABA and glycine, and each response was normalized to the mean of these two control measurements. Each point represents the mean of 4–7 (GABA, ●) or 3–11 (glycine, ○) observations. The continuous lines are the best fits of the data to the equation given in the Results. *B*, peak current response (normalized to cell capacitance) of GABA- and glycine-activated currents recorded in granule cells from rats aged 7, 12–15 or 20 days. Currents were recorded at −50 mV in response to 10 μM GABA (●; $n = 13$–78 cells) or 100 μM glycine (○; $n = 11$–51 cells). In *A* and *B*, S.E.M. are shown where larger than the symbols.

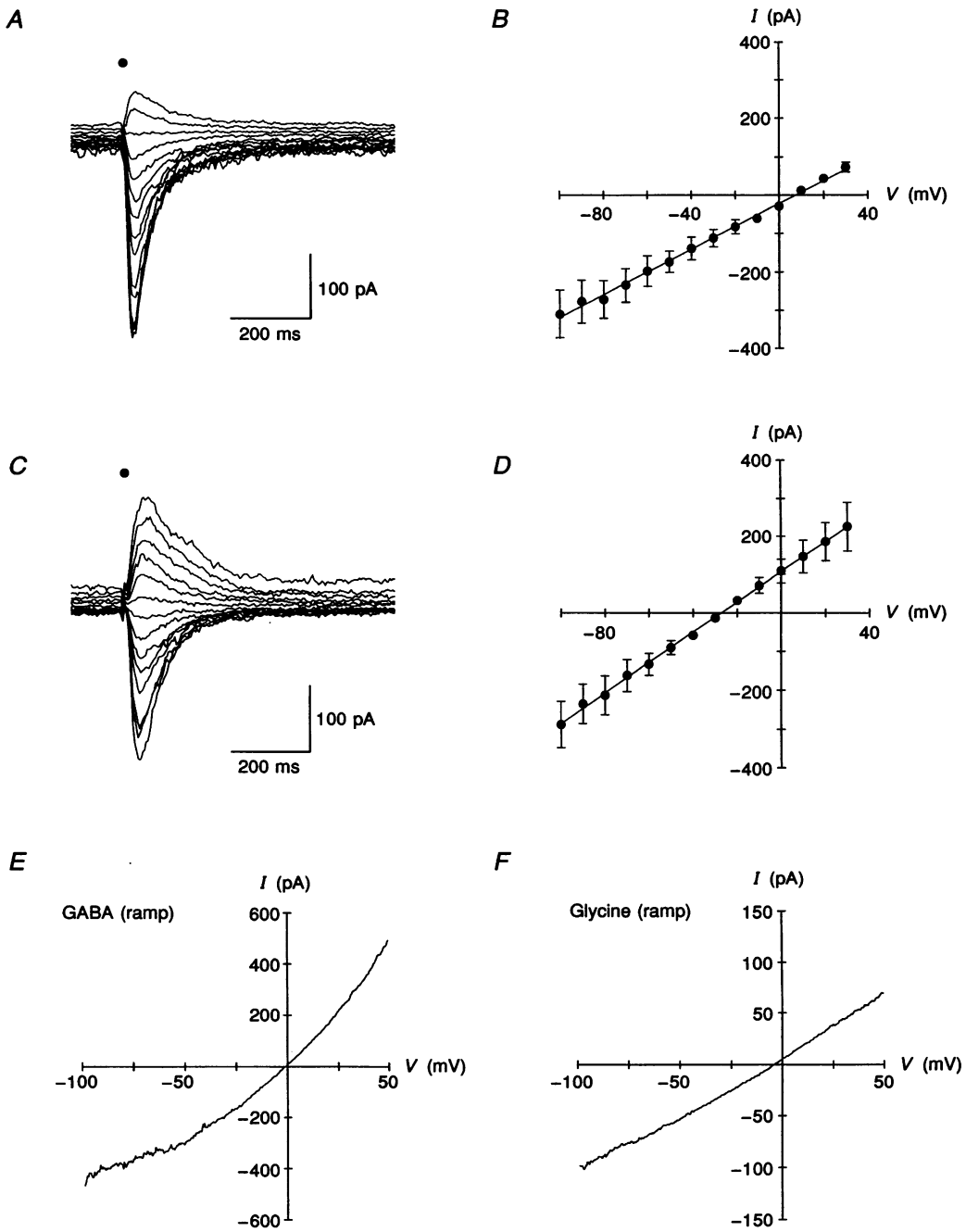

Figure 3. Current–voltage relationships of GABA- and glycine-evoked currents

A and *C*, families of whole-cell currents produced by the ionophoretic application of GABA at membrane potentials between −100 and 30 mV. GABA was applied for 10 ms at the point indicated (●). Each trace is the average of 3 applications. In *A* the internal solution contained CsCl ($[Cl^-]_i = 145$ mM, $[Cl^-]_o = 133{\cdot}5$ mM); in *C* the internal solution contained CsF ($[Cl]_i = 35$ mM, $[F^-]_i = 110$ mM, $[Cl^-]_o = 133{\cdot}5$ mM). *B* and *D*, current–voltage plots showing the relationship between peak GABA-induced current and membrane potential for currents recorded with the CsCl (*B*) or CsF internal (*D*). Each point represents the mean of measurements from 5 cells; S.E.M. are shown where larger than the symbol. The continuous lines through the points are least-squares linear regressions. Note the ~33 mV shift in reversal potential between *B* and *D*. *E* and *F*, representative GABA and glycine *I–V* curves produced by subtraction of ramp currents (−100 to 50 mV) recorded in the absence and presence of 10 μM GABA (*E*) or 100 μM glycine (*F*). The recordings are from two different granule cells (CsCl internal solution).

potential (Fig. 3*B*, mean of 5 cells) was linear and crossed the voltage axis at 6·3 ± 0·5 mV, close to the predicted Cl^- equilibrium potential under our recording conditions (E_{Cl} = 2·1 mV, calculated according to the Nernst equation using $[Cl^-]_i$ = 145 mM, $[Cl^-]_o$ = 133·5 mM). The ion selectivity of this response was investigated by replacing internal Cl^- with the relatively impermeant anion F^- (Bormann, Hamill & Sakmann, 1987; Fig. 3*C*). Changing from 145 mM Cl^- to 110 mM F^- (plus 35 mM Cl^-) shifted the reversal potential to −26·6 ± 1·3 mV (n = 5), as expected for a channel more permeable to Cl^- than F^- (Fig. 3*D*). This shift in reversal potential (32·9 mV) is close to that predicted (34·7 mV) by the Goldman–Hodgkin–Katz equation for this ionic substitution, assuming the permeability of F^-, relative to that of Cl^-, to be 0·02 (Bormann *et al.* 1987). Consideration of bicarbonate (HCO_3^-) permeability (0·18; Bormann *et al.* 1987) results in an exact correspondence of the observed and the predicted voltage shifts. In this case, the approximate intracellular concentration of HCO_3^- ($[HCO_3^-]_i$) was calculated from the extracellular HCO_3^- concentration ($[HCO_3^-]_o$, 26 mM), external proton concentration ($[H^+]_o$, 39·8 nM; pH 7·4) and internal proton concentration ($[H^+]_i$, 50·1 nM; pH 7·3), according to:

$$[HCO_3^-]_i = [HCO_3^-]_o \times [H^+]_o/[H^+]_i,$$

(Kaila & Voipio, 1990). However, it is unclear to what extent HCO_3^- can accumulate intracellularly, given the use of a HCO_3^--free pipette solution.

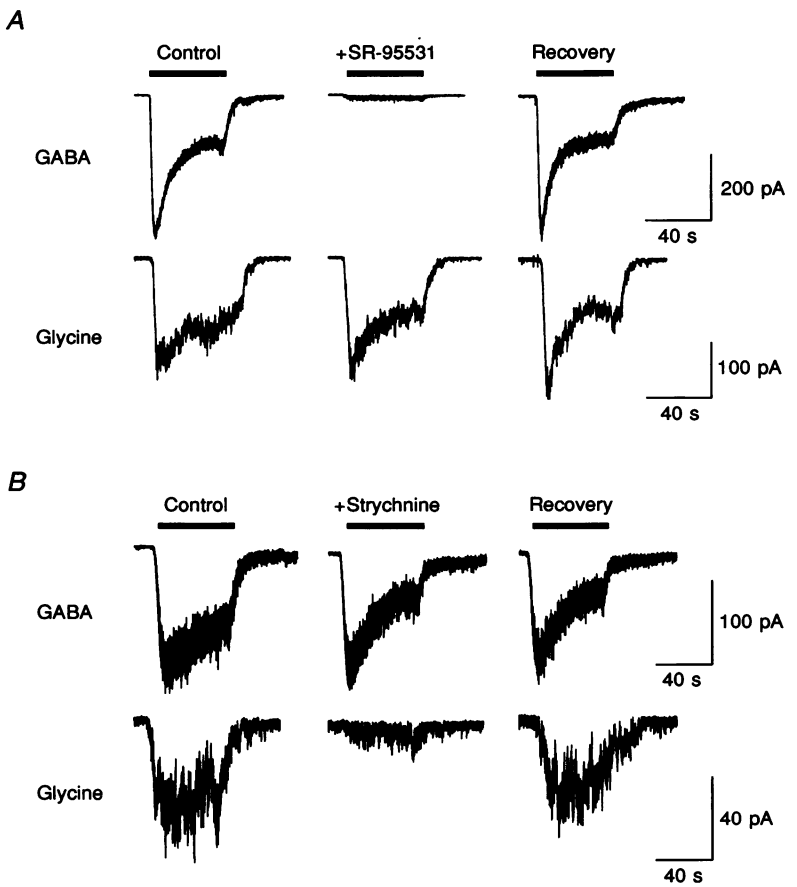

Figure 4. Antagonist pharmacology of GABA- and glycine-evoked currents

A, representative recordings from a single cell illustrating the selective block of GABA (10 μM) responses by SR-95531 (10 μM). *B*, recordings from a second cell illustrating the selective block of glycine (100 μM) responses by strychnine (200 nM). The cells were held at −50 mV. Each set of three traces shows the control whole-cell current response on the left, the response to agonist plus antagonist in the middle and a subsequent response to agonist alone on the right. Agonist applications were made at 3 min intervals. The bars above the traces indicate the duration of agonist application; SR-95531 and strychnine were perfused for 30 s prior to the application of GABA or glycine plus antagonist. A slight increase in the rate of desensitization of the GABA response with prolonged whole-cell recording was seen in a number of cells (e.g. *B*, upper panel) irrespective of their exposure to antagonists. This was not investigated further.

GABA I–V plots produced by ramp changes in holding potential (Fig. 3E) also reversed close to E_{Cl} (5·9 ± 1·1 mV, $n = 12$); however, in contrast with I–V plots obtained with ionophoretic application, they showed clear outward rectification. The ratio of chord conductances at +50 and −50 mV was 1·4 ± 0·04 ($n = 12$). Ramp I–V curves for glycine responses (Fig. 3F), recorded in a similar manner, also reversed close to E_{Cl} (−3·3 ± 3·0 mV, $n = 8$), but showed less evidence of outward rectification. Thus, for glycine, the ratio of chord conductances at +50 and −50 mV was 1·0 ± 0·2 ($n = 8$). As previously described, outward rectification of whole-cell GABA I–V relationships may reflect a voltage dependence of the channel gating reaction or of receptor desensitization (see, for example, Bormann *et al.* 1987; Weiss, 1988).

Antagonist pharmacology of GABA and glycine responses

To confirm that GABA and glycine responses arose from distinct receptor populations in these cells we examined the effects of the antagonists bicuculline, strychnine, picrotoxinin and SR-95531. Currents evoked by GABA (10 μM) were reversibly inhibited by bicuculline (3 μM; to 38·1 ± 5·3%, $n = 5$), SR-95531 (10 μM; to 0·7 ± 0·7%, $n = 4$) and picrotoxinin (100 μM; to 43·8 ± 9·7%, $n = 5$), but were unaffected by strychnine (200 nM). In contrast, responses to glycine (100 μM) were depressed by strychnine (200 nM; to 11·4 ± 1·6%, $n = 3$), but were unaffected by bicuculline (3 μM), SR-95531 (10 μM) or picrotoxinin (100 μM). Figure 4 illustrates the selective block of GABA and glycine responses by SR-95531 and strychnine, respectively. Although the selectivity of the antagonists we have examined is clearly not absolute (see, for example, Kaneda, Wakamori & Akaike, 1989), our results are qualitatively similar to those seen in other preparations, and suggest that GABA and glycine act on pharmacologically distinct receptor types in these cells.

GABA-activated single-channel currents

Figure 5A shows representative single-channel currents recorded from an outside-out patch exposed to 1 μM GABA (−60 mV). Channel openings to two current levels of 1·59 (left) and 1·09 pA (right) were observed, corresponding to single-channel chord conductances of 26·5 and 18·2 pS (for a reversal potential of 0 mV). The mean chord conductances of the single-channel events at −60 mV, determined from maximum likelihood fits of one or two Gaussian components to the distributions of channel amplitudes, were 15·8 ± 0·7 ($n = 5$) and 27·7 ± 0·5 pS ($n = 6$). The proportion of openings to each of these conductance levels

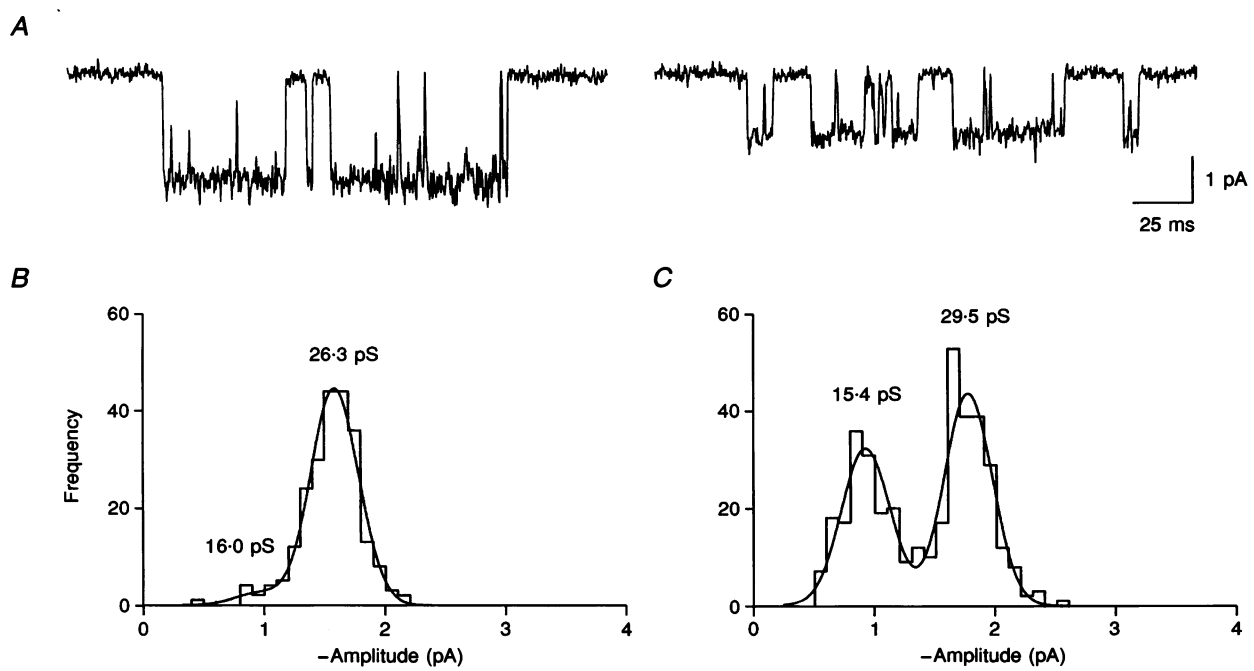

Figure 5. Single-channel currents activated by GABA

A, representative single-channel currents activated by 1 μM GABA in an outside-out membrane patch held at −60 mV (16-day-old animal). In this patch, openings to two levels were seen: 1·59 (left) and 1·09 pA (right). For display, traces were digitized at 5 kHz after low-pass filtering at 1 kHz. *B* and *C*, single-channel amplitude histograms from two different cells (16-day-old animals; −60 mV) illustrating the variable occurrence of the two current levels. In *B* the distribution is fitted with two Gaussian components with means of 0·96 (5·2%) and 1·58 pA (94·8%), corresponding to chord conductances of 16·0 and 26·3 pS. In *C* the distribution is fitted with two Gaussian components with means of 0·92 (42·6%) and 1·77 pA (57·4%), corresponding to chord conductances of 15·4 and 29·5 pS.

varied between patches. Examples of amplitude distributions from two patches which exhibited different proportions of '16' and '28 pS' openings are shown in Fig. 5*B* and *C*. In six patches (−60 mV), the proportion of openings to the 28 pS level was between 58 and 100% (mean, 82·8 ± 6·6%); both conductance levels were seen in five patches, while in one patch only the 28 pS level was present. This variation between patches in the occurrence of the two conductance levels, and the absence of clear transitions between levels, suggests that they may reflect the presence of two distinct channel types, rather than the activation of one channel type possessing two conductance states. A similar situation has been described for GABA-activated channels in patches from granule cells of the hippocampus (Edwards, Konnerth & Sakmann, 1990), where the mean single-channel conductances were 14 and 23 pS.

Distributions of apparent open times of all events contained two exponential components (not shown). For six patches analysed with a resolution of twice the filter rise time, the mean time constants (and relative areas) of these components were 0·62 ± 0·09 (85·3 ± 1·7%) and 4·5 ± 1·1 ms (14·7 ± 1·7%). Distributions of the lengths of the apparent openings, conditional on the amplitude of the openings, were also fitted with the sum of two exponential components. For openings to the 28 pS level, the time constants were 0·66 ± 0·1 (82·6 ± 2·2%) and 4·73 ± 1·13 ms (17·4 ± 2·2%, $n = 6$). For openings to the 16 pS level (in patches where more than 30% of the total openings were to this level), the time constants were 0·52 (68%) and 1·06 ms (32%, $n = 2$).

Glycine-activated single-channel currents

As glycine receptors occur at low density in granule cells we were unable to record single-channel currents in excised membrane patches. However, the small size and high input resistance of granule cells, together with the large conductance and slow kinetics of glycine channels, allowed us to record discrete single-channel activations in the whole-cell record in response to relatively low concentrations of glycine (10–30 μM). As shown in Fig. 6, channels activated by glycine exhibited multiple conductance levels and prolonged openings (up to several hundred milliseconds). Three conductance levels were detected: a main chord conductance of 55 pS (55·1 ± 0·8 pS, in 8 out of 8 cells), and less frequently

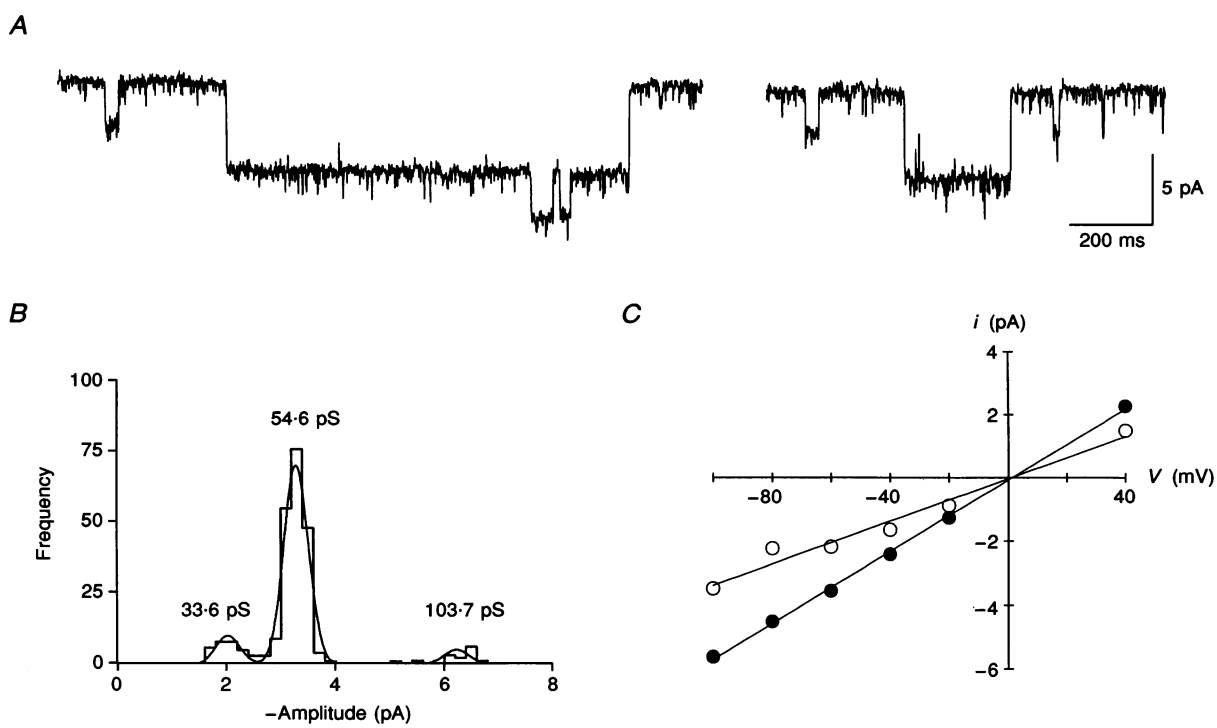

Figure 6. Single-channel currents activated by glycine

A, single-channel currents activated by 10 μM glycine recorded in the whole-cell configuration from a cell held at −60 mV. In this example, prolonged openings to a current level of 6·1 pA and briefer openings to 3·2 pA are present, two of which are superimposed upon a high-conductance event. For display, traces were digitized at 2 kHz after low-pass filtering at 1 kHz. *B*, an amplitude histogram from a second cell in which channel openings were to three current levels of 2·02 (11·9%), 3·28 (82·2%) and 6·22 pA (5·9%), corresponding to chord conductances of 33·6, 54·6 and 103·7 pS. *C*, an *i*–*V* plot for single-channel currents recorded from a different cell between −100 and 40 mV. The data were fitted by least-squares linear regression, yielding slope conductances of 37·0 (○) and 56·3 pS (●).

observed conductances of 104 pS (104·0 ± 0·9 pS, in 4 out of 8 cells) and 32 pS (32·1 ± 2·4 pS, in 7 out of 8 cells). A typical amplitude histogram from a cell exhibiting all three conductance levels is shown in Fig. 6*B*. The proportion of openings to each level varied from cell to cell. In this example, openings to the 32, 55 and 104 pS states comprised 11·9, 82·2 and 5·9% of the channel openings. At −60 mV, openings to the 55 pS level comprised 68·6–100% of all openings ($n = 8$); the corresponding values for the other levels were 0·4–31·4% for 32 pS ($n = 7$) and 5·9–23·1% for 104 pS ($n = 2$). Because of the apparently low glycine receptor density and the less than ideal signal-to-noise characteristics of the whole-cell recording, we were able to examine only a relatively small number of openings in each cell. The variability between cells in the proportion of openings to each conductance level may reflect this fact. In several cells where the channel amplitudes were measured over a range of potentials, the single-channel currents reversed direction near E_{Cl} (3·9 ± 0·9 mV, $n = 6$), as expected from the analysis of macroscopic whole-cell currents. Single-channel current–voltage ($i-V$) relationships were linear, with a slope conductance of the main state of 52·5 ± 1·3 pS ($n = 6$). Representative single-channel $i-V$ plots from a cell containing 32 and 55 pS openings are shown in Fig. 6*C*.

The prolonged openings of the 104 pS conductance states (see Fig. 6*A*) effectively excludes the possibility that these arise from superimposed 55 pS openings. Direct transitions between the different conductance levels were occasionally observed, but further analysis of this (and detailed kinetic

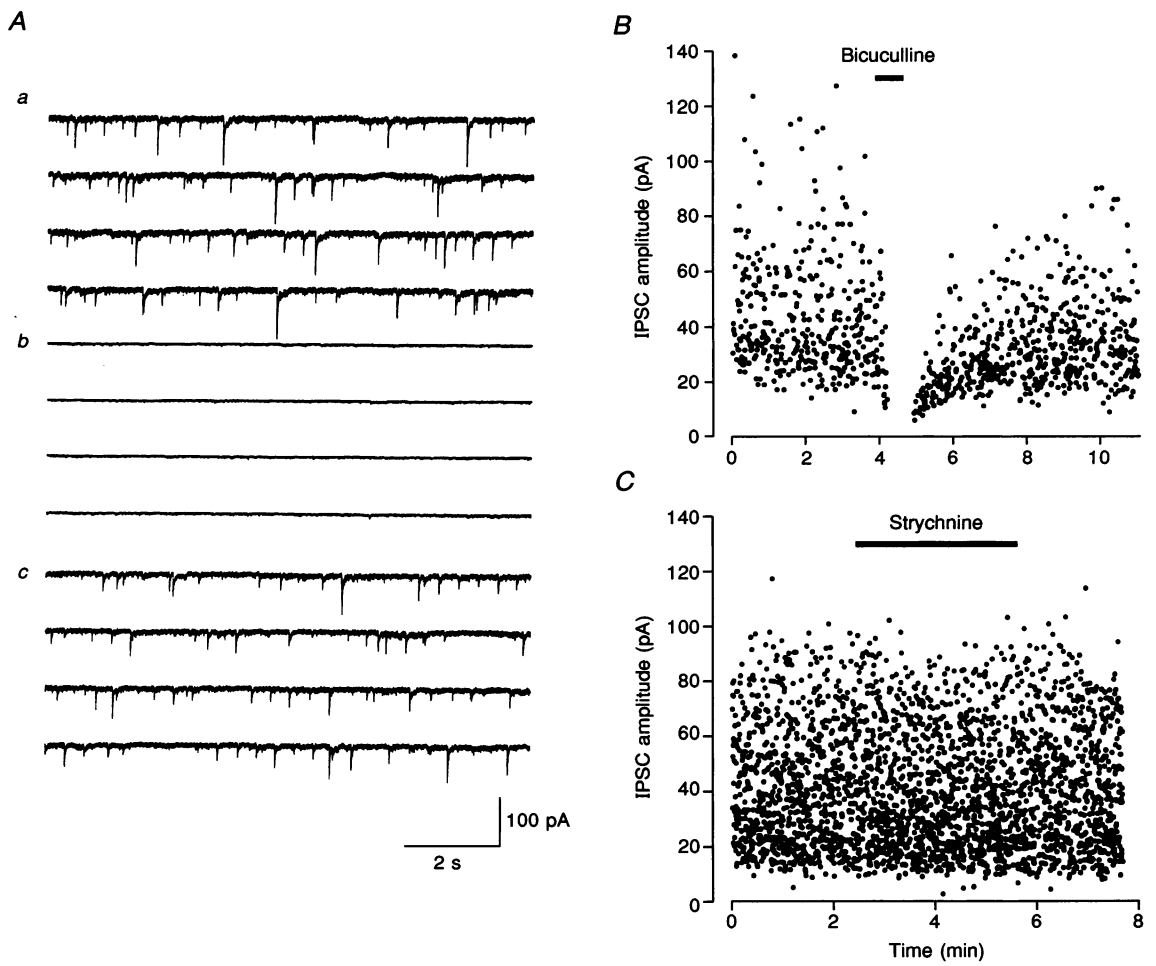

Figure 7. Block of spontaneous IPSCs by bicuculline

A a, consecutive records of spontaneous IPSCs recorded in the presence of 10 μM D-AP5 and 5 μM CNQX from a granule cell held at −60 mV (P12). *A b*, consecutive records obtained in the presence of 10 μM bicuculline. *A c*, synaptic currents recorded 2 min after the removal of bicuculline. The traces were low-pass filtered at 1 kHz and digitized at 5 kHz. *B*, a plot of IPSC amplitude against time, showing the complete block of IPSCs by bicuculline (same cell as *A*). The duration of bicuculline application is indicated by the horizontal bar. *C*, plot of IPSC amplitude against time for currents recorded from a different granule cell (P12). Application of 200 nM strychnine (indicated by the bar) had no effect on IPSC amplitude.

analysis) will require channels to be examined in excised patches. This may be possible in cells from younger animals, which exhibit a slightly higher glycine-activated current density (Fig. 2*B*). Cursor measurement of apparent open durations for each of the conductance levels gave values of 8·9 ± 0·8 ms for the 32 pS level (142 measured openings), 69·1 ± 2·8 ms for the 55 pS level (1056 openings) and 65·7 ± 15·3 ms for the 104 pS openings (24 openings). These values are approximate since brief events will inevitably be missed as a result of the additional filtering imposed by the whole-cell recording, and only a low number of measurements were possible for the infrequent 32 and 104 pS events. However, it is worth noting that the apparent open durations of the 55 and 104 pS states are considerably longer than the longest burst length of the 42 pS main-state of glycine-activated channels in cultured spinal neurones (Twyman & Macdonald, 1991).

Spontaneous IPSCs in granule cells

In the absence of TTX many granule cells exhibited spontaneous synaptic currents (66% of cells, $n = 88$), the frequency and amplitude (10–100 pA) of which varied considerably. The currents had a rapid rising phase (10–90% rise time, < 1 ms), and a decay that could be fitted with the sum of two exponential components (with time constants of approximately 10 and 40 ms at −60 mV; P12), having a variable contribution to the measured peak amplitude (see also Puia *et al.* 1994). With a CsCl-containing internal solution, the currents reversed direction near 0 mV ($E_{Cl} = 2·1$ mV). Replacing internal Cl^- with F^- (CsF-containing internal solution; see Methods) shifted the reversal potential to more negative values (around −30 mV), confirming that the principal charge carrier was Cl^-. The currents were unaffected by CNQX (5 μM) but were greatly reduced in frequency by TTX (300 nM), suggesting that they are spontaneous IPSCs resulting from the activity of Golgi interneurones. A more detailed description of the properties of these currents will be presented elsewhere.

As shown in Fig. 7, spontaneous IPSCs were rapidly and reversibly inhibited by bicuculline (10–15 μM; $n = 12$, P10–P15; Fig. 7*A* and *B*; see also Puia *et al.* 1994) or SR-95531 (10 μM; $n = 3$, P12, not shown) but were unaffected by 200 nM strychnine ($n = 3$, P12, Fig. 7*C*). In the presence of TTX, miniature IPSCs could be recorded at a very low frequency in some cells (M. Farrant & S. G. Cull-Candy, unpublished observation); these were also blocked by bicuculline.

Tonic activation of GABA receptors

As can be seen in Fig. 7, as well as blocking spontaneous synaptic currents, bicuculline markedly reduced the 'background' current noise. A persistent activation of GABA receptors could result from 'overspill' of synaptically released GABA onto extrasynaptic receptors (Isaacson, Solis & Nicoll, 1993) or tonic non-quantal release of GABA, as suggested for acetylcholine at the neuromuscular junction (Katz & Miledi, 1977). To investigate

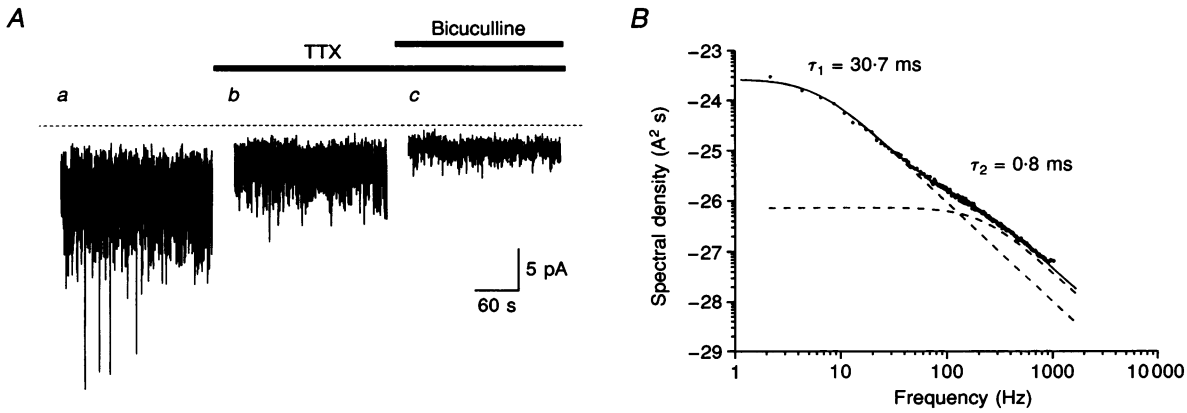

Figure 8. Background activity of GABA channels

A, whole-cell current recorded from a granule cell held at −60 mV. The current recorded under control conditions is shown on the left (*a*). Perfusion of 300 nM TTX (indicated by the horizontal bar) blocked spontaneous IPSCs and produced a small outward shift in the mean current level (*b*). The subsequent perfusion of 30 μM bicuculline reduced the amplitude of the residual current fluctuations and shifted the mean current level further (*c*). The zero-current level is indicated by the dashed line. Recordings *a*, *b* and *c* were separated by periods of approximately 40 s. For display, the current was filtered at 0·5 kHz and digitized at 20 ms per point. *B*, spectral analysis of GABA-induced current fluctuations. A net one-sided spectrum was obtained by subtracting the mean spectrum in the presence of 10 μM GABA from the mean control spectrum (−50 mV). The resulting spectrum was fitted with the sum of two Lorentzian curves with time constants of 0·8 and 30·7 ms for the fast and slow components, respectively.

these possibilities we made recordings in the presence of TTX (300 nM) which blocked nearly all synaptic activity in these cells. The subsequent addition of bicuculline (30 μM) reduced the background noise further and caused a small outward shift in the mean current, revealing the presence of residual current fluctuations not blocked by TTX (Fig. 8*A*). Addition of strychnine (1 μM) or D-AP5 (20 μM) plus CNQX (5 μM) did not produce any further change in the background current, indicating the absence of tonic activation of glycine or glutamate receptors (tonic activation of NMDA receptors is seen in these cells in the absence of extracellular Mg^{2+}; Farrant *et al.* 1994).

Fluctuation analysis of the bicuculline-sensitive current yielded spectra that could be fitted with the sum of two Lorentzian curves, having half-power frequencies (f_{c1} and f_{c2}) of $18{\cdot}1 \pm 6{\cdot}5$ and $261{\cdot}5 \pm 58{\cdot}0$ Hz ($n = 4$). The corresponding values of τ_{noise}, which represent the mean lifetime (or burst lengths) of the underlying channels, were $0{\cdot}82 \pm 0{\cdot}31$ and $15{\cdot}09 \pm 6{\cdot}17$ ms for the fast and slow components, respectively. The mean channel conductance estimated from the spectra was $13{\cdot}7 \pm 1{\cdot}6$ pS (for a reversal potential of 5·9 mV, determined from ramp *I–V* relationships). These values are very similar to those obtained from the analysis of GABA-induced current fluctuations (Fig. 8*B*). In this case, the half-power frequencies were $9{\cdot}8 \pm 2{\cdot}1$ and $225{\cdot}9 \pm 36{\cdot}8$ Hz ($n = 4$), corresponding to τ_{noise} values of $0{\cdot}75 \pm 0{\cdot}10$ and $18{\cdot}9 \pm 4{\cdot}14$ ms. The mean channel conductance estimated from the spectra was $15{\cdot}3 \pm 3{\cdot}6$ pS, and from plots of the variance of the current fluctuations (σ^2) *versus* the mean current amplitude (μ_I) was $17{\cdot}0 \pm 3{\cdot}7$ pA ($n = 4$). These conductance estimates are similar to that previously obtained from fluctuation analysis of GABA-evoked currents in cerebellar granule cells in culture (16 pS; Cull-Candy & Ogden, 1985). Together, these results suggest that the bicuculline-sensitive 'background' current in these cells can be ascribed to tonic, presumably non- quantal, release of GABA. Although it is difficult to exclude the possibility of GABA release from damaged neurones, a 'background' activity of GABA channels was more apparent in cells receiving inhibitory input (as judged by the presence of IPSCs), in keeping with the idea of GABA 'leakage' from Golgi cell terminals.

'Excitatory' effects of GABA and glycine

In some cells, examined in the absence of TTX, the application of glycine, or low concentrations of GABA, produced a marked increase in the frequency of spontaneous synaptic currents ($n = 6$, P12). In the example illustrated in Fig. 9*B*, 100 μM glycine increased the frequency of synaptic events from approximately 0·2 to 2 Hz in the absence of any clear 'postsynaptic' response. In the same cell, 3 μM GABA produced a similar, although slightly less dramatic effect on the frequency of synaptic currents, which were superimposed on a sustained inward current (Fig. 9*A*). The increase in synaptic activity was rapidly reversed when the agonist was removed. Similar results were seen with glycine in five cells (P12). The synaptic currents evoked in this way had a time course similar to that of spontaneous inhibitory currents in these cells, and were similarly eliminated by bicuculline (10 μM, $n = 3$). The effects of GABA and glycine persisted in the presence of CNQX (5 μM) and D-AP5 (10 μM), but were abolished by TTX (300 nM). Together these data suggest that the GABA- and glycine-evoked synaptic currents are GABAergic IPSCs arising from regenerative currents in Golgi interneurones. We have not investigated the

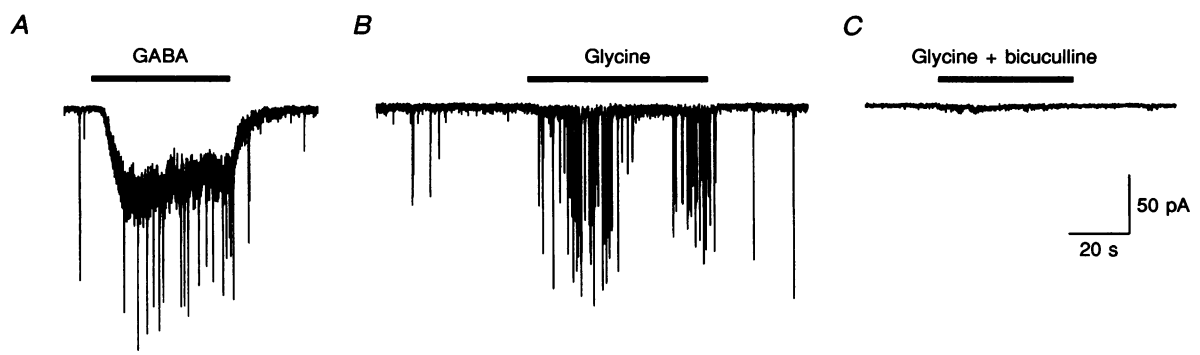

Figure 9. 'Excitatory' effects of GABA and glycine

A, whole-cell current recorded from a granule cell held at −50 mV. Application of 10 μM GABA in the absence of TTX produced an inward current and increased the frequency of IPSCs, which are seen superimposed on the postsynaptic response. *B*, in the same cell, application of 100 μM glycine produced a very small inward current but dramatically increased the frequency of IPSCs. *C*, in the same cell, perfusion of 10 μM bicuculline eliminated all spontaneous IPSCs and prevented the responses to glycine (and GABA, not shown). The bars above each trace indicate the duration of agonist application. In *C*, bicuculline was perfused for 1 min prior to the application of glycine.

mechanism of this 'excitatory' effect further. Higher concentrations of GABA (10 μM and above), giving rise to larger postsynaptic responses, produced a less clear 'excitatory' effect and often caused a reduction in IPSC frequency following their application.

DISCUSSION

Our data show that granule cells in thin cerebellar slices from the rat express both GABA- and glycine-activated Cl^--selective channels with different single-channel properties, coupled to pharmacologically distinct receptors. Overall, our findings accord with the results of previous studies demonstrating the presence within the granule cell layer of mRNAs encoding various $GABA_A$ (Laurie, Seeburg & Wisden, 1992) and glycine (Malosio, Marqueze Pouey, Kuhse & Betz, 1991) receptor subunits, and the immunohistochemical demonstration of GABA (Somogyi, Takagi, Richards & Möhler, 1989; Baude, Sequier, McKernan, Olivier & Somogyi, 1992) and glycine (Triller *et al.* 1987) receptor proteins on the surface of granule cells. Although previous reports have described GABA-activated currents in cultured cerebellar granule cells (Cull-Candy & Ogden, 1985; Vicini *et al.* 1986; Kilić *et al.* 1993; Robello *et al.* 1993; Maconochie *et al.* 1994), glycine-activated channels have not previously been described in these cells.

Properties of GABA-activated currents

Whole-cell responses to GABA were found to be Cl^- dependent and selectively blocked by the antagonists bicuculline, SR-95531 and picrotoxinin, as expected for the activation of $GABA_A$ receptors. These features are similar to those described for granule cells from P0–P10 animals maintained in culture for 1–21 days (Kilić *et al.* 1993; Robello *et al.* 1993; Maconochie *et al.* 1994). The greatest variation among previous reports, and between these and the present study, lies in the parameters derived from the analysis of GABA concentration– response curves. Estimates for the GABA EC_{50} vary between 2·3 and 20·7 μM for cultured granule cells (Robello *et al.* 1993; Kilić *et al.* 1993) and 45 μM for granule cells in the slice (present study). Also, our estimate of 0·94 for the Hill coefficient is slightly lower than the values of 1·2 (Robello *et al.* 1993) and 1·48 (Kilić *et al.* 1993) described for whole-cell GABA responses recorded from cultured cells, although a second population of cells with a Hill coefficient of 0·94 was also described by Kilić *et al.* (1993). While this disparity may reflect a difference in receptor properties, it could also arise from differences in the speed of GABA application and a variable extent of GABA uptake, both of which may be affected by the local density of cells, which will differ between dissociated cultures and an intact slice. In a recent study in which these problems were obviated, Maconochie *et al.* (1994) used a rapid application method to record GABA-activated currents in membrane patches excised from cultured granule cells. The authors observed a half-maximal current at approximately 10 μM GABA and a Hill coefficient for the 'on rate' of the current response of 1·6, suggesting that the binding of more than one GABA molecule is required for receptor activation.

GABA receptor single-channel properties

A range of single-channel conductances have been described for $GABA_A$ receptors in vertebrate neurones. In most cases between two and five conductance levels are seen, with a main state of approximately 20 (Weiss, Barnes & Hablitz, 1988; Edwards *et al.* 1990) or 26–31 pS (Bormann *et al.* 1987; Huck & Lux, 1987; Llano, Marty, Johnson, Ascher & Gähwiler, 1988; Macdonald, Rogers & Twyman, 1989; Smith, Zorec & McBurney, 1989; Mistry & Hablitz, 1990; Newland, Colquhoun & Cull-Candy, 1991; Smart, 1992; Kilić *et al.* 1993). Our analysis of GABA-activated single-channel currents in cerebellar granule cells revealed the presence of two conductance states: 16 and 28 pS, similar to those of 18–20 and 28–31 pS observed in cerebellar interneurones (Huck & Lux, 1987), Purkinje cells (Llano *et al.* 1988; Smart, 1992) and granule cells (Kilić *et al.* 1993) in culture.

Direct transitions between different current levels in the single-channel record (Smith *et al.* 1989; Mistry & Hablitz, 1990; Newland *et al.* 1991; Smart, 1992) may be taken as evidence for the presence of a single GABA channel capable of adopting multiple conductance states, rather than the existence of several channels with different conductances or the superimposed openings of channels. In the present study, however, the failure to observe clear sublevel transitions and the variable occurrence of the 16 and 28 pS states in different membrane patches is suggestive of the existence of two distinct channel types. In this regard, it is interesting to note the biexponential decay of IPSCs in these cells (this study; Puia *et al.* 1994) and the comparable biexponential decay of currents resulting from the brief application of GABA to nucleated granule cell patches (Puia *et al.* 1994). Such macroscopic current behaviour may result from the activation of two channel types with different kinetic properties, but further study, including analysis of burst properties of the single-channel currents, will be required in order to address this issue.

Comparison with recombinant $GABA_A$ receptors

Cerebellar granule cells in the adult rat contain mRNAs for a variety of $GABA_A$ receptor subunits, those for $\alpha1$, $\alpha6$, $\beta2$, $\beta3$, $\gamma2$ and δ being most abundant, with lower levels of $\alpha4$, $\beta1$ and $\gamma3$ (see Laurie *et al.* 1992). During the early postnatal period, mRNAs for $\alpha2$, $\alpha3$ and $\gamma1$ are also present (see Laurie, Wisden & Seeburg, 1992). The single-channel properties of only a few of the many possible combinations of these subunits have been examined in heterologous expression systems, so it is difficult at present to draw any firm conclusion regarding the likely

composition of the $GABA_A$ receptors recorded in this study. Nevertheless, a number of points are of interest. Whereas, the co-expression of α-, β- and γ-subunits gives rise to receptors with main conductances of 29–33 pS (Verdoorn, Draguhn, Ymer, Seeburg & Sakmann, 1990; Angelotti & Macdonald, 1993; Verdoorn, 1994), combinations of α- and β-subunits produce channels with lower conductances (11–18 pS; Verdoorn *et al.* 1990; Angelotti & Macdonald, 1993). Thus, the predominant conductance of 28 pS seen in the present study suggests that neonatal granule cells express a receptor isoform containing a γ-subunit. This idea is supported by our observation that during the first two postnatal weeks granule cell IPSCs and whole-cell responses to GABA can be potentiated by the benzodiazepine flurazepam (see also Puia *et al.* 1994), since only those receptors containing a γ-subunit are modulated by benzodiazepine agonists (for review see Wisden & Seeburg, 1992).

In the adult rat, the granule cell layer of the cerebellum exhibits relatively little [^{3}H]benzodiazepine binding (Sieghart, Eichinger, Richards & Möhler, 1987). This is thought to reflect the high level of expression by granule cells of the α6-subunit (Lüddens *et al.* 1990; Laurie *et al.* 1992; Baude *et al.* 1992). When co-expressed together with β- and γ-subunits, the α6-subunit forms atypical receptors that are insensitive to benzodiazepine agonists such as diazepam, but which have a high affinity for the partial inverse agonist Ro 15-4513 (Lüddens *et al.* 1990). Messenger RNA encoding the α6 subunit is detectable in granule cells after the first postnatal week, but maximal levels are not reached until postnatal day 21 (Zheng, Santi, Bovolin, Marlier & Grayson, 1994). This coincides with our observation that benzodiazepine potentiation is restricted to the first and second postnatal weeks. Also, the main single-channel conductance of 28 pS seen during this period clearly differs from that of the only α6-containing recombinant receptor examined to date (~34 pS for $\alpha6\beta1\gamma2$; Angelotti, Tan, Chahine & Macdonald, 1992). However, no single-channel data are available for other α6-containing combinations, such as the $\alpha6\alpha1\beta2$(or $\beta3$)$\gamma2s\gamma2L$ complex recently identified by immunoprecipitation studies and suggested to form a major subpopulation diazepam-insensitive [^{3}H]Ro 15-4513 binding sites in cerebellar granule cells (Khan, Gutierrez & De Blas, 1994). Further comparison of recombinant receptors with native channels recorded from animals of different ages will be required to establish the type(s) of GABA receptors expressed in these cells.

Properties of glycine-activated currents

Several observations indicate that GABA and glycine activate pharmacologically and functionally distinct receptors. Glycine-activated currents were blocked by a low concentration of strychnine but were unaffected by the GABA antagonists bicuculline and SR-95531. The two receptor types also appear to be subject to different regulatory processes, since currents evoked by glycine were maintained in the absence of ATP, in marked contrast to the decline of GABA responses (see also Song & Huang, 1990; Vaello, Ruiz-Gomez, Lerma & Mayor, 1994). Furthermore, there are clear conductance and kinetic differences in the single-channel currents. Channels activated by glycine opened to three conductance states (32, 55 and 104 pS), with most openings being to the 55 pS level. A wide range of multiple conductances (12–94 pS) have been described for glycine-activated channels in other mammalian neurones (Bormann *et al.* 1987; Huck & Lux, 1987; Smith *et al.* 1989; Takahashi & Momiyama, 1991; Twyman & Macdonald, 1991; Takahashi, Momiyama, Hirai, Hishinuma & Akagi, 1992). Although our results broadly correspond with this range, there are several differences worth noting. Firstly, the conductance of 104 pS is larger than values previously reported for native glycine receptors. Secondly, the 55 pS main-conductance state is also somewhat larger than that observed in other cells (42–48 pS). Finally, we did not detect either of the two lower conductance states (12–14 and 19–21 pS) seen in other studies (Bormann *et al.* 1987; Smith *et al.* 1989; Takahashi & Momiyama, 1991); however, given that our recordings were made in the whole-cell configuration, we cannot exclude entirely the possible existence of lower conductance states.

Comparison with recombinant glycine receptors

In situ hybridization studies have revealed a surprisingly widespread distribution of glycine receptor α- and β-subunit mRNAs in the mammalian brain. In neonatal rats, the granule cell layer of the cerebellum contains only α2- and β-transcripts (Malosio *et al.* 1991). Thus the glycine responses we have recorded could result from the activation of homomeric α2-receptors, heteromeric $\alpha2/\beta$-receptors or a mixture of both (β-subunits alone do not form functional channels; see Bormann, Rundström, Betz & Langosch, 1993). Three lines of evidence suggest that the channels present in granule cells are most likely to be $\alpha2/\beta$-hetero-oligomers. Firstly, expression of α-subunit cDNAs alone results in channels that can be blocked by picrotoxinin; heteromeric receptors containing the β-subunit are 50- to 200-fold less sensitive (Pribilla, Takagi, Langosch, Bormann & Betz, 1992). In the present study, whole-cell currents activated by glycine (100 μM) were unaffected by picrotoxinin (100 μM). Secondly, co- expression of the β-subunit with any α-subunit markedly decreases the main-state conductance of the homomeric channel. In the case of α2, this conductance is decreased from 111 to 54 pS in the presence of a β-subunit (Bormann *et al.* 1993). Not only does this $\alpha2/\beta$ main conductance agree with that seen here (55 pS), but the two additional conductances of 112 pS

(11% of openings) and 36 pS (14%) seen with $\alpha 2/\beta$-receptors (Bormann *et al.* 1993) are also similar to those of 104 and 32 pS we have recorded in granule cells. Finally, the Hill coefficient for heteromeric receptors is lower than that for homomeric α-receptors (e.g. 2·5 *versus* 4·2 for $\alpha 1/\beta$- and $\alpha 1$-receptors, respectively; Bormann *et al.* 1993) and more closely matches that seen in the present study (2·6; Fig. 2*A*).

Functional significance of granule cell glycine receptors

Glycine-activated currents have not previously been described in cerebellar granule cells, although responses to glycine have been observed in other cerebellar neurones, including dissociated Purkinje neurones (Kaneda, Nakamura & Akaike, 1988), presumptive Purkinje neurones in culture (Mori-Okamoto & Tatsuno, 1985; Cull-Candy & Usowicz, 1989) and unidentified interneurones in culture (Huck & Lux, 1987). Recently, glycine-activated currents were observed following injection into *Xenopus* oocytes of poly(A)$^+$ mRNA from granule cell cultures (Wahl, Elster & Schousboe, 1994). In the present study, responses to 100 μM glycine were seen in approximately half of the granule cells examined. This heterogeneity may reflect different developmental states of individual cells.

It is clear from this study that glycine receptors, although present in granule cells, are not activated synaptically. Spontaneous IPSCs could be completely blocked by bicuculline or SR-95531, indicating that Golgi cell–granule cell transmission is mediated by GABA (see also Puia *et al.* 1994). What then is the role of glycine receptors in these cells? Glycine is traditionally considered as an inhibitory neurotransmitter. However, the effects of glycine, like those of GABA, depend on the chloride equilibrium potential and the resting membrane potential of the cell. In fetal and neonatal neurones, activation of a chloride conductance by GABA (Ben-Ari, Cherubini, Corradetti & Gaiarsa, 1989) or glycine (Ito & Cherubini, 1991) causes membrane depolarization which may lead to an elevation of intracellular calcium (Connor, Tseng & Hockenberger, 1987; Reichling, Kyrozis, Wang & MacDermott, 1994). Whether glycine and GABA produce similar effects in neonatal granule cells is unknown, but a depolarizing action on immature Golgi interneurones is one possible explanation for the increase in IPSC frequency produced by these agonists (high concentrations of GABA, which failed to alter IPSC frequency, may increase Golgi cell conductance sufficiently to shunt any excitatory effect). Since granule cells express GABA and glycine receptors during the period of mossy-fibre and Golgi cell synapse formation, activation of these receptors by GABA or glycine released from developing Golgi cell terminals could serve a neurotrophic role in dendritic elaboration or formation of the synaptic glomerulus. Of course, it remains to be seen under what circumstances Golgi cell terminals might release glycine, and whether this can result in the activation of glycine receptors in granule cells.

Angelotti, T. P. & Macdonald, R. L. (1993). Assembly of $GABA_A$ receptor subunits: $\alpha_1\beta_1$ and $\alpha_1\beta_1\gamma_{2s}$ subunits produce unique ion channels with dissimilar single-channel properties. *Journal of Neuroscience* **13**, 1429–1440.

Angelotti, T. P., Tan, F., Chahine, K. G. & Macdonald, R. L. (1992). Molecular and electrophysiological characterization of a allelic variant of the rat $\alpha 6$ $GABA_A$ receptor subunit. *Molecular Brain Research* **16**, 173–178.

Araki, T., Yamano, M., Murakami, T., Wanaka, A., Betz, H. & Tohyama, M. (1988). Localization of glycine receptors in rat central nervous system: an immunocytochemical analysis using monoclonal antibody. *Neuroscience* **2**, 613–624.

Baude, A., Sequier, J.-M., McKernan, R. M., Olivier, K. R. & Somogyi, P. (1992). Differential subcellular distribution of the $\alpha 6$ subunit *versus* the $\alpha 1$ and $\beta 2/3$ subunits of the $GABA_A$/benzodiazepine receptor complex in granule cells of the cerebellar cortex. *Neuroscience* **51**, 739–748.

Beattie, C. E. & Siegel, R. E. (1993). Developmental clues modulate $GABA_A$ receptor subunit mRNA expression in cultured cerebellar granule neurons. *Journal of Neuroscience* **13**, 1784–1792.

Ben-Ari, Y., Cherubini, E., Corradetti, R. & Gaiarsa, J. L. (1989). Giant synaptic potentials in immature rat CA3 hippocampal neurones. *Journal of Physiology* **416**, 303–325.

Bisti, S., Iosif, G., Marchesi, G. F. & Strata, P. (1971). Pharmacological properties of inhibitions in the cerebellar cortex. *Experimental Brain Research* **14**, 24–37.

Bormann, J., Hamill, O. P. & Sakmann, B. (1987). Mechanism of anion permeation through channels gated by glycine and γ-aminobutyric acid in mouse cultured spinal neurones. *Journal of Physiology* **385**, 243–286.

Bormann, J., Rundström, N., Betz, H. & Langosch, D. (1993). Residues within transmembrane segment M2 determine chloride conductance of glycine receptor homo- and hetero-oligomers. *EMBO Journal* **12**, 3729–3737.

Bovolin, P., Santi, M. R., Puia, G., Costa, E. & Grayson, D. (1992). Expression patterns of γ-aminobutyric acid type A receptor subunit mRNAs in primary cultures of granule neurons and astrocytes from neonatal rat cerebella. *Proceedings of the National Academy of Sciences of the USA* **89**, 9344–9348.

Chen, Q. X., Stelzer, A., Kay, A. R. & Wong, R. K. (1990). $GABA_A$ receptor function is regulated by phosphorylation in acutely dissociated guinea-pig hippocampal neurones. *Journal of Physiology* **420**, 207–221.

Colquhoun, D. & Sigworth, F. J. (1983). Fitting and statistical analysis of single channel records. In *Single-channel Recording*, ed. Sakmann, B. & Neher, E., pp. 191–263. Plenum Press, New York.

Connor, J. A., Tseng, H. Y. & Hockenberger, P. E. (1987). Depolarization- and transmitter-induced changes in intracellular Ca^{2+} of rat cerebellar granule cells in explant culture. *Journal of Neuroscience* **7**, 1384–1400.

CULL-CANDY, S. G. & OGDEN, D. C. (1985). Ion channels activated by L-glutamate and GABA in cultured cerebellar neurons of the rat. *Proceedings of the Royal Society* B **224**, 367–373.

CULL-CANDY, S. G. & USOWICZ, M. M. (1989). Whole-cell current noise produced by excitatory and inhibitory amino acids in large cerebellar neurones of the rat. *Journal of Physiology* **415**, 533–553.

EDWARDS, F. A., KONNERTH, A. & SAKMANN, B. (1990). Quantal analysis of inhibitory synaptic transmission in the dentate gyrus of rat hippocampal slices: a patch-clamp study. *Journal of Physiology* **430**, 213–249.

FARRANT, M. & CULL-CANDY, S. G. (1991). Excitatory amino acid receptor-channels in Purkinje cells in thin cerebellar slices. *Proceedings of the Royal Society* B **244**, 179–184.

FARRANT, M., FELDMEYER, D., TAKAHASHI, T. & CULL-CANDY, S. G. (1994). NMDA-receptor channel diversity in the developing cerebellum. *Nature* **368**, 335–339.

GYENES, M., FARRANT, M. & FARB, D. H. (1988). "Run-down" of γ-aminobutyric $acid_A$ receptor function during whole-cell recording: a possible role for phosphorylation. *Molecular Pharmacology* **34**, 719–723.

HUCK, S. & LUX, H. D. (1987). Patch-clamp study of ion channels activated by GABA and glycine in cultured cerebellar neurons of the mouse. *Neuroscience Letters* **79**, 103–107.

ISAACSON, J. S., SOLIS, J. M. & NICOLL, R. A. (1993). Local and diffuse synaptic actions of GABA in the hippocampus. *Neuron* **10**, 165–175.

ITO, S. & CHERUBINI, E. (1991). Strychnine-sensitive glycine responses of neonatal rat hippocampal neurones. *Journal of Physiology* **440**, 67–83.

KAILA, K. & VOIPIO, J. (1990). GABA-activated bicarbonate condutance: influence on E_{GABA} and on postsynaptic pH regulation. In *Chloride Channels and Carriers in Nerve, Muscle, and Glial Cells*, ed. ALVAREZ-LEEFMANS, F. J. & RUSSELL, J. M., pp. 331–352. Plenum, New York.

KANEDA, M., FARRANT, M. & CULL-CANDY, S. G. (1994). GABA- and glycine-activated currents in granule cells of the rat cerebellum. *Journal of Physiology* **476**, 68*P*.

KANEDA, M., NAKAMURA, H. & AKAIKE, N. (1988). Mechanical and enzymatic isolation of mammalian CNS neurons. *Neuroscience Research* **5**, 299–315.

KANEDA, M., WAKAMORI, M. & AKAIKE, N. (1989). GABA-induced chloride current in rat isolated Purkinje cells. *American Journal of Physiology* **256**, C1153–1159.

KATZ, B. & MILEDI, R. (1977). Transmitter leakage from motor nerve endings. *Proceedings of the Royal Society* B **196**, 59–72.

KHAN, Z. U., GUTIERREZ, A. & DE BLAS, A. L. (1994). The subunit composition of a $GABA_A$/benzodiazepine receptor from rat cerebellum. *Journal of Neurochemistry* **63**, 371–374.

KILIĆ, G., MORAN, O. & CHERUBINI, E. (1993). Currents activated by GABA and their modulation by Zn^{2+} in cerebellar granule cells in culture. *European Journal of Neuroscience* **5**, 65–72.

LAURIE, D. J., SEEBURG, P. H. & WISDEN, W. (1992). The distribution of 13 $GABA_A$ receptor subunit mRNAs in the rat brain. II. Olfactory bulb and cerebellum. *Journal of Neuroscience* **12**, 1063–1076.

LAURIE, D. J., WISDEN, W. & SEEBURG, P. H. (1992). The distribution of 13 $GABA_A$ receptor subunit mRNAs in the rat brain. III. Embryonic and postnatal development. *Journal of Neuroscience* **12**, 4151–4172.

LLANO, I., MARTY, A., JOHNSON, J. W., ASCHER, P. & GAHWILER, B. H. (1988). Patch-clamp recording of amino acid-activated responses in 'organotypic' slice cultures. *Proceedings of the National Academy of Sciences of the USA* **85**, 3221–3225.

LÜDDENS, H., PRITCHETT, D. B., KÖHLER, M., KILLISCH, I., KEINÄNEN, K., MONYER, H., SPRENGEL, R. & SEEBURG, P. H. (1990). Cerebellar $GABA_A$ receptor selective for a behavioural alcohol antagonist. *Nature* **346**, 648–651.

MACDONALD, R. L., ROGERS, C. J. & TWYMAN, R. E. (1989). Kinetic properties of the $GABA_A$ receptor main conductance state of mouse spinal cord neurones in culture. *Journal of Physiology* **410**, 479–499.

MACONOCHIE, D. J., ZEMPEL, J. M. & STEINBACH, J. H. (1994). How quickly can $GABA_A$ receptors open? *Neuron* **12**, 61–71.

MALOSIO, M. L., MARQUEZE POUEY, B., KUHSE, J. & BETZ, H. (1991). Widespread expression of glycine receptor subunit mRNAs in the adult and developing rat brain. *EMBO Journal* **10**, 2401–2409.

MISTRY, D. K. & HABLITZ, J. J. (1990). Activation of subconductance states by γ-aminobutyric acid and its analogs in chick cerebral neurons. *Pflügers Archiv* **416**, 454–461.

MORALES, E. & TAPIA, R. (1987). Neurotransmitters of the cerebellar glomeruli: uptake and release of labelled gamma-aminobutyric acid, glycine, serotonin and choline in a purified glomerulus fraction and in granular layer slices. *Brain Research* **420**, 11–21.

MORI-OKAMOTO, J. & TATSUNO, J. (1985). Development of sensitivity to GABA and glycine in cultured cerebellar neurons. *Brain Research* **352**, 249–258.

NEWLAND, C. F., COLQUHOUN, D. & CULL-CANDY, S. G. (1991). Single channels activated by high concentrations of GABA in superior cervical ganglion neurones of the rat. *Journal of Physiology* **432**, 203–233.

OTTERSEN, O. P., STORM-MATHISEN, J. & SOMOGYI, P. (1988). Colocalization of glycine-like and GABA-like immunoreactivities in Golgi cell terminals in the rat cerebellum: a postembedding light and electron microscopic study. *Brain Research* **450**, 342–353.

PRIBILLA, I., TAKAGI, T., LANGOSCH, D., BORMANN, J. & BETZ, H. (1992). The atypical M2 segment of the beta subunit confers picrotoxinin resistance to inhibitory glycine receptor channels. *EMBO Journal* **11**, 4305–4311.

PUIA, G., COSTA, E. & VICINI, S. (1994). Functional diversity of GABA-activated Cl^- currents in Purkinje *versus* granule neurons in rat cerebellar slices. *Neuron* **12**, 117–126.

REICHLING, D. B., KYROZIS, A., WANG, J. & MACDERMOTT, A. B. (1994). Mechanisms of GABA and glycine depolarization-induced calcium transients in rat dorsal horn neurons. *Journal of Physiology* **476**, 411–421.

ROBELLO, M., AMICO, C. & CUPELLO, A. (1993). Regulation of $GABA_A$ receptor in cerebellar granule cells in culture: differential involvement of kinase activities. *Neuroscience* **53**, 131–138.

SIEGHART, W., EICHINGER, A., RICHARDS, J. G. & MÖHLER, H. (1987). Photoaffinity labelling of benzodiazepine receptor proteins with the partial inverse agonist [^{3}H]Ro 15-4513: a biochemical and autoradiographic study. *Journal of Neurochemistry* **48**, 46–52.

SILVER, R. A., TRAYNELIS, S. F. & CULL-CANDY, S. G. (1992). Rapid-time-course miniature and evoked excitatory currents at cerebellar synapses in situ. *Nature* **355**, 163–166.

SMART, T. G. (1992). A novel modulatory binding site for zinc on the $GABA_A$ receptor complex in cultured rat neurones. *Journal of Physiology* **447**, 587–625.

SMITH, S. M., ZOREC, R. & MCBURNEY, R. N. (1989). Conductance states activated by glycine and GABA in rat cultured spinal neurones. *Journal of Membrane Biology* **108**, 45–52.

SOMOGYI, P., TAKAGI, H., RICHARDS, J. G. & MÖHLER, H. (1989). Subcellular localization of benzodiazepine/$GABA_A$ receptors in the cerebellum of rat, cat, and monkey using monoclonal antibodies. *Journal of Neuroscience* **9**, 2197–2209.

SONG, Y. M. & HUANG, L. Y. (1990). Modulation of glycine receptor chloride channels by cAMP-dependent protein kinase in spinal trigeminal neurons. *Nature* **348**, 242–245.

STELZER, A., KAY, A. R. & WONG, R. K. (1988). $GABA_A$-receptor function in hippocampal cells is maintained by phosphorylation factors. *Science* **241**, 339–341.

TAKAHASHI, T. & MOMIYAMA, A. (1991). Single-channel currents underlying glycinergic inhibitory postsynaptic responses in spinal neurons. *Neuron* **7**, 965–969.

TAKAHASHI, T., MOMIYAMA, A., HIRAI, K., HISHINUMA, F. & AKAGI, H. (1992). Functional correlation of fetal and adult forms of glycine receptors with developmental changes in inhibitory synaptic receptor channels. *Neuron* **9**, 1155–1161.

THOMPSON, C. L. & STEPHENSON, F. A. (1994). $GABA_A$ receptor subtypes expressed in cerebellar granule cells: a developmental study. *Journal of Neurochemistry* **62**, 2037–2044.

TRILLER, A., CLUZEAUD, F. & KORN, H. (1987). γ-Aminobutyric acid-containing terminals can be apposed to glycine receptors at central synapses. *Journal of Cell Biology* **104**, 947–956.

TWYMAN, R. E. & MACDONALD, R. L. (1991). Kinetic properties of the glycine receptor main- and sub-conductance states of mouse spinal cord neurones in culture. *Journal of Physiology* **435**, 303–331.

VAELLO, M.-L., RUIZ-GÓMEZ, A., LERMA, J. & MAYOR, F. JR (1994). Modulation of inhibitory glycine receptors by phosphorylation by protein kinase C and cAMP-dependent protein kinase. *Journal of Biological Chemistry* **269**, 2002–2008.

VERDOORN, T. A. (1994). Formation of heteromeric γ-aminobutyric acid type A receptors containing two different α subunits. *Molecular Pharmacology* **45**, 475–480.

VERDOORN, T. A., DRAGUHN, A., YMER, S., SEEBURG, P. H. & SAKMANN, B. (1990). Functional properties of recombinant $GABA_A$ receptors depend on subunit composition. *Neuron* **4**, 919–928.

VICINI, S., WROBLEWSKI, J. T. & COSTA, E. (1986). Pharmacological modulation of GABAergic transmission in cultured cerebellar neurons. *Neuropharmacology* **25**, 207–211.

WAHL, P., ELSTER, L. & SCHOUSBOE, A. (1994). Identification and function of glycine receptors in cultured cerebellar granule cells. *Journal of Neurochemistry* **62**, 2457–2463.

WEISS, D. S. (1988). Membrane potential modulates the activation of GABA-gated channels. *Journal of Neurophysiology* **59**, 514–527.

WEISS, D. S., BARNES, E. M. JR & HABLITZ, J. J. (1988). Whole-cell and single-channel recordings of GABA-gated currents in cultured chick cerebral neurons. *Journal of Neurophysiology* **59**, 495–513.

WILKIN, G. P., CSILLAG, A., BALÁZS, R., KINGSBURY, A. E., WILSON, J. E. & JOHNSON, A. L. (1981). Localization of high affinity [^{3}H]glycine transport sites in the cerebellar cortex. *Brain Research* **216**, 11–33.

WISDEN, W. & SEEBURG, P. H. (1992). $GABA_A$ receptor channels from subunits to functional entities. *Current Opinion in Neurobiology* **2**, 263–269.

YUSTE, R. & KATZ, L. C. (1991). Control of postsynaptic Ca^{2+} influx in developing neocortex by excitatory and inhibitory neurotransmitters. *Neuron* **6**, 333–344.

ZARBIN, M. A., WAMSLEY, J. K. & KUHAR, M. J. (1981). Glycine receptor: light microscopic autoradiographic localization with [^{3}H]strychnine. *Journal of Neuroscience* **1**, 532–547.

ZHENG, T., SANTI, M.-R., BOVOLIN, P., MARLIER, L. N. J.-L. & GRAYSON, D. R. (1993). Developmental expression of the α6 $GABA_A$ receptor subunit mRNA occurs only after cerebellar granule cell migration. *Developmental Brain Research* **75**, 91–103.

Acknowledgements

We would like to thank Beverley Clark, Dirk Feldmeyer, Akiko Momiyama, Angus Silver and Tomoyuki Takahashi for comments on the manuscript, and David Colquhoun and Steve Traynelis for providing software. This work was supported by the Medical Research Council, the Wellcome Trust, the Howard Hughes Medical Institute (International Scholars Award to S.G.C.-C.) and the Ciba-Geigy Foundation (Japan) for the Promotion of Science (M.K.).

Author's present address

M. Kaneda: Department of Physiology, Yamagata University School of Medicine, Yamagata 990-23, Japan.

Received 20 July 1994; accepted 22 November 1994.